**Online supplemental materials for**

# Synergistic therapeutic combination with a CAF inhibitor enhances CAR-NK-mediated cytotoxicity via reduction of CAF-released IL-6

Young Eun Lee†, Ga-Yeon Go†, Eun-Young Koh†, Han-Na Yoon, Minkoo Seo, Seung-Mo Hong, Ji Hye Jeong, Jin-chul Kim, Duck Cho, Tae Sung Kim, Song Cheol Kim*, Eunsung Jun*, and Mihue Jang*

## Supplemental methods

### Isolation and characterization of CAFs from human tumor tissues.

Fresh tumor tissues were obtained from surgical specimens of patients diagnosed with PDAC, which were immediately soaked in RPMI640 media (Sigma-Aldrich Corp, St. Louis, MO, USA), and transferred to the laboratory within 30 min. Tumor tissues were rinsed with phosphate-buffered saline (PBS) in a clean bench, minced into < 2 $mm^3$ fragments, and digested with 0.1 % (W/V) collagenase type 1 (Gibco, Grand Island, NY, USA) at 37°C for 20 min. The resulting fragments were centrifuged at 200 × *g* for 5 min, washed with PBS, plated onto DMEM media (11965-092, Gibco) containing 10% fetal bovine serum (FBS) (10270-098, Gibco) and 1% penicillin/ streptomycin (15140-122, Gibco), and allowed to adhere.[1] After incubation of cultured cells with the anti-human EpCAM-FITC antibody (clone 9C4, Biolegend, San Diego, CA, USA), EpCAM negative cells were sorted using the BD FACS Canto™ II system (BD Biosciences, SJ, California, USA), followed by culturing, while fibroblasts were maintained in DMEM media containing 10% FBS and 1% penicillin/ streptomycin at 37 °C in a humidified atmosphere with 5% $CO_2$. For the characterization of CAFs, FACS analysis was performed with the following antibodies; anti-human EpCAM-FITC (Clone 9C4, Biolegend), anti-human FAP-PE (Clone 427819, R&D Systems, Minneapolis, MN, USA), anti-human α-SMA-APC (Clone 1A4, R&D Systems), anti-human IL6-PE/Cyanine7 (clone MQ2-13A5, Biolegend), anti-human CD126 (IL6Rα)-PE (clone UV4, Biolegend), anti-human CD130 (gp130)-APC (clone 2E1B02, Biolegend), anti-human Mesothelin-PE (clone 420411, R&D Systems), IgG1 Alexa Fluor® 488-conjugated antibody (clone 11711, R&D Systems), IgG1κ Isotype-PE antibody (clone MOPC-21, Biolegend), IgG1κ Isotype-PE/Cyanine7 antibody (clone RTK2071, Biolegend), $IgG_{2A}$ Isotype-Alexa Fluor® 647-conjugated antibody (clone 20102, R&D Systems), and $IgG_{2A}$ Isotype-PE

antibody (clone 54447, R&D Systems). For intracellular staining of CD126 (IL6Rα), the cells were permeabilized with eBioscience™ IC Fixation Buffer (Invitrogen™ 00-8222-49) and eBioscience™ Permeabilization Buffer (10X) (Invitrogen™ 00-8333-56) before incubation with antibodies.

**Cell culture**

Capan2 and MIA PaCa-2 were cultured in McCoy's 5A medium (Welgene, Daegu, Korea) and Dulbecco's Modified Eagle's Medium (DMEM, Welgene), respectively, supplemented with 10 % FBS (Welgene) and 1 % antibiotic antimycotic solution (Welgene). Patient-derived CAF cells were maintained in RPMI 1640 medium (Welgene) supplemented with 10 % FBS (Welgene) and 1 % antibiotic antimycotic solution (Welgene). NK92 cells were purchased from the American Type Culture Collection (ATCC, USA). NK92 cells were grown in minimum essential medium (MEM) α (Gibco) supplemented with 20 % FBS (Gibco), 10 × MEM vitamin solution (Gibco), 0.1 mM 2-mercaptoethanol (Gibco), 1 % penicillin/streptomycin (Gibco), and rhIL-2 (R&D systems; 200 IU/mL) at 37 °C under a humidified atmosphere with 5 % $CO_2$. Frozen PBMCs, which were purchased from Lonza Inc. (Walkersville, MD, USA), were used for PBNK expansion. PBNK cells were expanded with 100 Gy-irradiated K562 feeder cells for 2-3 weeks according to our previous protocol.[2] In this study, membrane-bound IL-18/21-overexpressiong K562 feeder cells were used.[3]

**Selection of anti-fibrotic drugs**

Nintedanib (S1010, Selleck chemicals LLC, Houston, TX, USA), SOM230 (24092, Cayman Chemical, Ann Arbor, MI, USA) and Metformin (PHR1084, Sigma-Aldrich, USA) were purchased from the regarding vendors. Nintedanib, SOM230, or Metformin was added to

each five types of CAFs at the indicated concentrations for 72 h. Nintedanib was also used in Capan2 and MIA PaCa2 cancer cells under the same conditions. Percentage of cell proliferation on CAFs in response to different treatment conditions was evaluated using the EZ-Cytox cell viability assay kit (DoGenBio, Seoul, Korea) 72 h post treatment according to the manufacturer's instructions. 10 ng/ml of PDGF-AA and/or PDGF-BB (PeproTech, USA) were treated to evaluate viability in the presence or absence of nintedanib. Additionally, the morphology of CAFs under treatment with nintedanib was visualized by optical microscopy (Olympus, Tokyo, Japan).

**Western blot analysis**

Cell lysates containing a protease inhibitor cocktail (Roche, Mannheim, Germany) were electrophoresed on SDS-PAGE gels and separated proteins were then transferred to nitrocellulose membranes. Membranes were blocked with 5 % skimmed milk in Tris-buffered saline (TBS-T, 0.1 % Tween-20) for 1 h at 25 °C, and then incubated with the primary antibodies against FAP (Abcam, Cambridge, UK), a-SMA (Proteintech, Rosemont, IL, USA), pPDGFRβ (CST, Danvers, MA, USA), PDGFRβ (CST), pVEGFR2 (CST), VEGFR2 (CST), pFGFR1 (CST), FGFR1 (CST), pAKT (CST), AKT (CST), pERK (CST), ERK (CST), IL-6 (abcam), cleaved Caspase-3 (CST), β-actin (Santa Cruz Biotechnology, CA, USA), and HSP90 (Santa Cruz Biotechnology) overnight at 4 °C. Membranes were washed and then incubated with horse radish peroxidase (HRP) conjugated, species-specific secondary antibody at 25 °C, and then rewashed. For protein detection, HRP signals were visualized using ChemiDoc (Bio-Rad, Hercules, CA, USA), followed by detection using the chemiluminescence method (Bio-Rad). Full western blots are shown in online supplemental figure S21and S22.

**Viability test on PDGFRβ K.O CAFs**

For generation of PDGFRβ K.O CAFs, 400 pmol of each PDGFRβ-targeting sgRNAs were mixed with 24.4 pmol of spCas9 (IDT, USA) for 20min at room temperature to make Cas9 RNP solution. CAF cells treated with Cas9 RNP solution (online supplemental table S5) were electroporated at 1700 V for 20ms and one pulse using a Neon Electroporator (Invitrogen, USA). For viability tests, K.O cells were treated with 3 μM of nintedanib in the presence or absence of 10 ng/ml of PDGF ligand AB and BB for 72 h at 37 °C. Viability was analyzed using an EZ-Cytox cell viability assay kit according to the manufacturer`s instructions.

**Measurement of annexin V influx**

RFP-CAF cells or GFP-Capan2 cells were seeded in μ-slide 8 well (ibidi, USA). Next day, cells were washed with PBS buffer and then nintedanib was incubated at the indicated concentration. To analyze the apoptotic efficacy, RFP-CAF cells were stained with annexin V-BUV395 (BD) and visualized using a LionheartFX automated live cell microscope (BioTek, Bad Friedrichshall, Germany) at 24h post-treatment. GFP-Capan2 cells were stained with annexin V-APC (Biolegend), and then flow cytometry was performed on a Cytoflex (Beckman Coulter) and data were analyzed using FlowJo (BD).

**Harvesting conditioned media from CAF**

CAF cells were cultured with or without nintedanib for 72 h at 37 °C under a humidified atmosphere with 5 % $CO_2$. Then, conditioned media were harvested by removing cells.

**T cell activation analysis**

Jurkat T cells were incubated in the conditioned media from CAF in the presence or absence of nintedanib for 6 h. Then, cells were harvested and washed with PBS buffer. Cells were stained with CD69-APC (FN50) antibody. The CD69 expression was assessed by flowcytometry.

**Formation of tumor-CAF coculture spheroids**

Capan2 cells and CAF cells were seeded at a ratio of 1:1 in 96-well Black/Clear Round Bottom Ultra-Low Attachment Spheroid Microplates (Corning, NY, USA) and centrifuged at 1350 rpm for 3 min. Cells were then incubated for 24 h at 37 °C under a humidified atmosphere with 5 % $CO_2$. For evaluation of NK-mediated killing, NK92 or PBNK cells were subsequently incubated at the indicated E:T ratios after formation of tumor-CAF spheroids.

**Live cell imaging**

For visualization, GFP- and RFP-carrying lentiviruses were transduced in Capan2 and CAFs, respectively. Then, Capan2-CAF spheroids were cocultured with NK92 cells in the presence or absence of nintedanib. Each mono spheroid (Capan2 or CAF only, respectively) and double co-culture (CAF spheroid-NK92 or Capan2 spheroid-NK92, respectively) were tested as controls. Real-time fluorescence images were obtained at 37 °C under a humidified atmosphere with 5 % $CO_2$, using a LionheartFX automated live cell microscope. For time-dependent NK-mediated killing, images were captured at 4 h intervals for 48 h. Image processing and relative intensity or area calculation were performed using the Gen5 Software (BioTeck).

**Next-generation sequencing (NGS) analysis**

For transcriptomic analysis, CAF and Capan2 were treated with 3 μM nintedanib or not, respectively. At 72 h post treatment, total RNA was extracted from each indicated group of cells. The whole transcriptome sequencing and data analysis were performed by E-Biogen Inc. (Seoul, Korea). DEGs were analyzed using the FC value of 2 and a p-value of < 0.05.

**NK functional studies**

To conduct flow cytometric analysis, NK92 or PBNK cells were incubated in the presence or absence of nintedanib either in *in-vitro* spheroid coculture system or alone. After harvest at 24 or 48 h, cells were stained in PBS containing 0.5 % BSA and 0.05 % azide. For intracellular staining, cells were fixed and permeabilized using cytofix/cytoperm (BD Biosciences). Dead cells were excluded by staining with the LIVE/DEAD Fixable Dead Viability Dye (Thermo Fisher Scientific, Cleveland, OH, USA). The antibodies used in this study were purchased from Biolegend: NKp30-PerCP/Cy5.5 (P30-15), NKp44-APC (P44-8), NKp46-PE/Dazzle™ 594 (9E2), CD69-PE/Cy7 (FN50), DNAM-1-Brilliant Violet 421™ (11A8), and Perforin-PE (dG9). NKG2C-Alexa Fluor® 700 (134591) was purchased from R&D Systems. Flow cytometry was performed on a Cytoflex (Beckman Coulter) and data were analyzed using FlowJo (BD). To test the flow cytometry-based cancer killing efficacy, propodium iodide- (PI, Invitrogen, Carlsbad, CA, USA) or 7-aminoaactinomycin D- (7-AAD, Biolegend) stained dead cells were analyzed in the NK-excluded population.

For assessment of NK-mediated cytotoxicity, NanoLuc luciferase-expressing Capan2 cells were co-cultured with PBNK or CAR-NK cells under treatment conditions that included nintedanib, IL-6, and anti-IL-6 antibody for 24 h. After washing, a cytotoxicity assay was performed using the Nano-Glo® Luciferase Assay System (Promega, Madison, WI, USA).

**Lentivirus production and transduction**

For construction of a second generation CAR-expressing plasmid, each DNA fragment encoding the SFFV promoter and CAR including SS1 scFv was synthesized from Cosmo Genetech (Seoul, Korea), respectively. The GFP-expressing DNA fragment was obtained from PCR amplification using specific primers. Three DNA fragments were inserted into an EcoR1/EcoRV (NEB, USA)-cut pCDH lentivirus vector (Addgene, Cambridge, MA, USA, #72266) using the NEBuilder HiFi DNA assembly kit (NEB, Ipswich, MA, USA).

For the generation of genetically engineered NK cells, CAR expressing shuttle vector, psPAX2 packaging vector, and Baboon envelope vector were transfected on HEK293T cells[4]. Lentiviral supernatants were collected at 24 and 48 h, and then the virus was concentrated using the Lenti-X concentrator (TaKaRa, Tokyo, Japan). NK92 cells were transduced with MOI 100 of MSLN-CAR lentivirus. MSLN-CAR-expressing NK92 were sorted by a MA900 Cell Sorter (SONY, Toyko, Japan).

**Human cytokine and growth factor arrays**

For human cytokine and growth factor arrays, CAF cells were treated in the presence or absence of 3 μM nintedanib, and then, their conditioned media were harvested after 48 or 72 h. Analysis of human cytokines and growth factors was performed using the Human Cytokine array C3 (RayBiotech, Atlanta, GA, USA) and Human Growth factor array C1 (Raybiotech), respectively, according to the manufacturer's instructions. Membranes were detected using ChemiDoc.

**Quantitative real-time (qRT) PCR**

CAF cells were incubated in the presence or absence of nintedanib, and then total RNA was extracted using an RNeasy mini kit (QIAGEN, Hilden, Germany) and reverse-transcribed into cDNA using a SuperiorScript III Reverse Transcriptase (Thermo Fisher Scientific) as per

the manufacturer's protocols. qRT PCR was performed on a StepOnePlus Real-Time PCR System (Applied Biosystems, Foster City, CA, USA) using SYBR Green Master Mix (Roche). Specific amplicons were obtained using specific target primers. Primers used in qRT-PCR are listed in online supplemental table S4.

**Analysis of hematological toxicity**

Blood of mice was taken from the abdominal vein. This procedure was performed in triplicate. For chemical analysis, 500 μL of blood was centrifuged for 15 min at 3000 rpm and 4 °C, and the plasma was carefully transferred to collection tubes. The levels of aspartate aminotransferase (AST), alanine aminotransferase (ALT), total protein (TP), blood urea nitrogen (BUN), and creatinine (Cr) were analyzed using the Advia 120 Hematology analyzer (Bayer Healthcare, Myerstown, PA, USA).[5]

**Establishment and characterization of human PDAC organoid**

To generation of luciferase-expressing organoids, a AsPC1 cell line containing the luciferase gene (AsPC1_luc cell line) was subcutaneously transplanted into nude mice, and then, the organoid was generated using tumor tissue from mice xenografts. The generated organoid was named ASPC1_XO. For establishment of a fluorescence tagged PDAC organoid, a patient-derived organoid (Og-AMC-363) was electroporated using the Neon™ electroporation system (Invitrogen) according to the manufacturer's instructions.[6] Briefly, Og-AMC-363 was electroporated with pLentiGuide-puro-mCherry (Addgene, #117986) and selected by puromycin-containing (1 ug/ml) media. The selected organoids were sorted following expression of mcherry by FACS Aria (BD Bioscience, San Jose, CA, USA) and seeded in BME. To determine the characterization of the generated organoids, they were examined by histology (H&E) and morphology (bright field image).[7] mCherry expression of

Og-AMC-363 was confirmed by fluorescence microscopy, and whole exome sequencing (WES) analysis was performed. ASPC1_XO was treated with luciferin (BioVison, No.7902-1, Milpitas, CA, USA), and the luminescence signal was determined using a VICTOR3™ instrument (PerkinElmer, Waltham, MA, USA).

**CAR-PBNK-mediated killing, based on a PDAC organoid/CAFs co-culture system**

To generate the co-culture model based on organoids, PDAC organoid with CAFs and PBNK (or CAR-PBNK) were cultured at a 1:1:4 ratio (PDAC organoid; $5x10^3$cells/100ul, CAFs; $5x10^3$ cells/100ul, PBNK: $2x10^4$ cells/100ul).[8] The mixture was suspended in PDAC organoid culture media containing IL-2 (200 IU/ml) and seeded on a 96-well plate, under various conditions including nintedanib and anti-IL-6R blocking antibody (MedChemExpress, USA) for 48 h. Bright field- or fluorescence images were obtained using Eclipse Ts2 (Nikon Instruments, Tokyo, Japan) at 10x magnification. To evaluate CAR-PBNK efficacy on the co-culture model based on PDAC organoids, the viability of ASPC1_XO and Og-AMC-363 was determined by luminescence and fluorescence, respectively. In brief, relative luminescence unit (RFU) of the luciferin-treated ASPC1_XO was measured using VICTOR3™ (PerkinElmer). The fluorescence of Og-AMC-363 was imaged by an IVIS® instrument (PerkinElmer). The ROI of images was analyzed using the Living Image® 4.7.2 software and calculated after subtracting the background signal.[9] To analyze the CAR-PBNK efficacy, the luminescence or fluorescence signals of the residual organoids were measured under different conditions based on the ROIs or RFU.

**The transcriptomic-based public data set of pancreatic cancer**

Transcriptomics data of pancreatic cancer in the TCGA database were downloaded from the cBioportal database (https://cbioportal-

datahub.s3.amazonaws.com/paad_tcga_pan_can_atlas_2018.tar.gz.). For Kaplan–Meier survival analysis, the 177 patient cohort from the PanCancer dataset was divided into two groups depending on the level of expression of MSLN, PDGFRβ and IL-6.[10]

**Statistical analysis**

All data represent the mean and standard error of the mean from at least three independent experiments. Survival analysis using the Kaplan-Meier method with the log-rank test was performed using the Statistical Package for the Social Sciences (SPSS) version 21.0 (IBM Corp., Armonk, NY, USA). The p-value was derived from one-way ANOVA followed by multiple comparison tests using the GraphPad prism 9 software (San Diego, CA, USA). A *P*-value <0.05(*), <0.01 (**), < 0.001(***), or < 0.0001(***) was considered statistically significant. NS indicates not significant.

**References**

1. Kim MJ, Kim MS, Kim SJ, et al. Establishment and characterization of 6 novel patient-derived primary pancreatic ductal adenocarcinoma cell lines from Korean pancreatic cancer patients. Cancer Cell Int. 2017;17:47. doi: 10.1186/s12935-017-0416-8.
2. Lee YE, Yuk CM, Lee M, et al. Facile discovery of a therapeutic agent for NK-mediated synergistic antitumor effects using a patient-derived 3D platform. Biomater Sci. 2022;10(3):678-691. doi: 10.1039/d1bm01699g.
3. Thangaraj JL, Phan MT, Kweon S, et al. Expansion of cytotoxic natural killer cells in multiple myeloma patients using K562 cells expressing OX40 ligand and membrane-bound IL-18 and IL-21. Cancer Immunol Immunother. 2022;71(3):613-625. doi: 10.1007/s00262-021-02982-9.
4. Girard-Gagnepain A, Amirache F, Costa C, et al. Baboon envelope pseudotyped LVs outperform VSV-G-LVs for gene transfer into early-cytokine-stimulated and resting HSCs. Blood. 2014;124(8):1221-31. doi: 10.1182/blood-2014-02-558163.
5. Jun E, Kim SC, Lee CM, et al. Synergistic effect of a drug loaded electrospun patch and systemic chemotherapy in pancreatic cancer xenograft. Sci Rep. 2017;7(1):12381. doi: 10.1038/s41598-017-12670-3.

6. Martens YA, Xu S, Tait R, et al. Generation and validation of APOE knockout human iPSC-derived cerebral organoids. STAR Protoc. 2021;2(2):100571. doi: 10.1016/j.xpro.2021.100571.
7. Seino T, Kawasaki S, Shimokawa M, et al. Human Pancreatic Tumor Organoids Reveal Loss of Stem Cell Niche Factor Dependence during Disease Progression. Cell Stem Cell. 2018;22(3):454-467 e6. doi: 10.1016/j.stem.2017.12.009.
8. Schnalzger TE, de Groot MH, Zhang C, et al. 3D model for CAR-mediated cytotoxicity using patient-derived colorectal cancer organoids. EMBO J. 2019;38(12). doi: 10.15252/embj.2018100928.
9. Luli S, Di Paolo D, Perri P, et al. A new fluorescence-based optical imaging method to non-invasively monitor hepatic myofibroblasts in vivo. J Hepatol. 2016;65(1):75-83. doi: 10.1016/j.jhep.2016.03.021.
10. Butera A, Roy M, Zampieri C, et al. p53-driven lipidome influences non-cell-autonomous lysophospholipids in pancreatic cancer. Biol Direct. 2022;17(1):6. doi: 10.1186/s13062-022-00319-9.

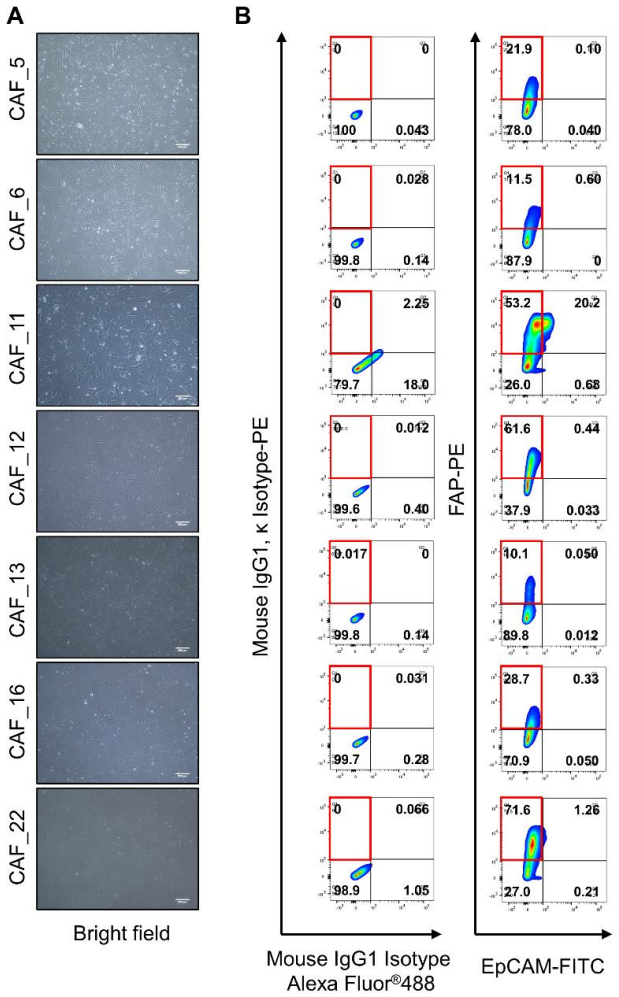


**Supplemental Figure 1.** Characterization of PDAC-derived CAFs. (a) Optical images showing primary fibroblasts cultured from tumor tissues of patients with PDAC. Scale bars indicate 250 μm. (b) Representative FACS profiling was conducted to confirm the CAF population. FAP and EpCAM were used as fibroblast and epithelial cell markers, respectively.

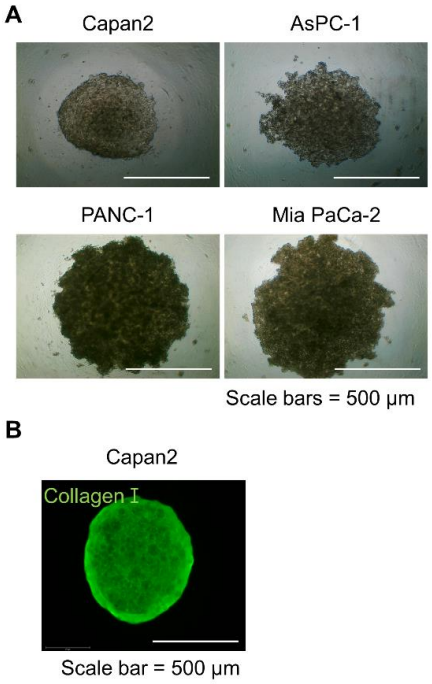


**Supplemental Figure 2.** Spheroid formation of pancreatic cancer cell lines. (A) Optical images exhibiting the spheroid morphology of different cancer cells, including Capan2, AsPC-1, PANC-1, and Mia PaCa-2 at a density of $1 \times 10^5$ cells/well. (B) The expression of Collagen I was detected in a Capan2 spheroid, as indicated by green fluorescence.

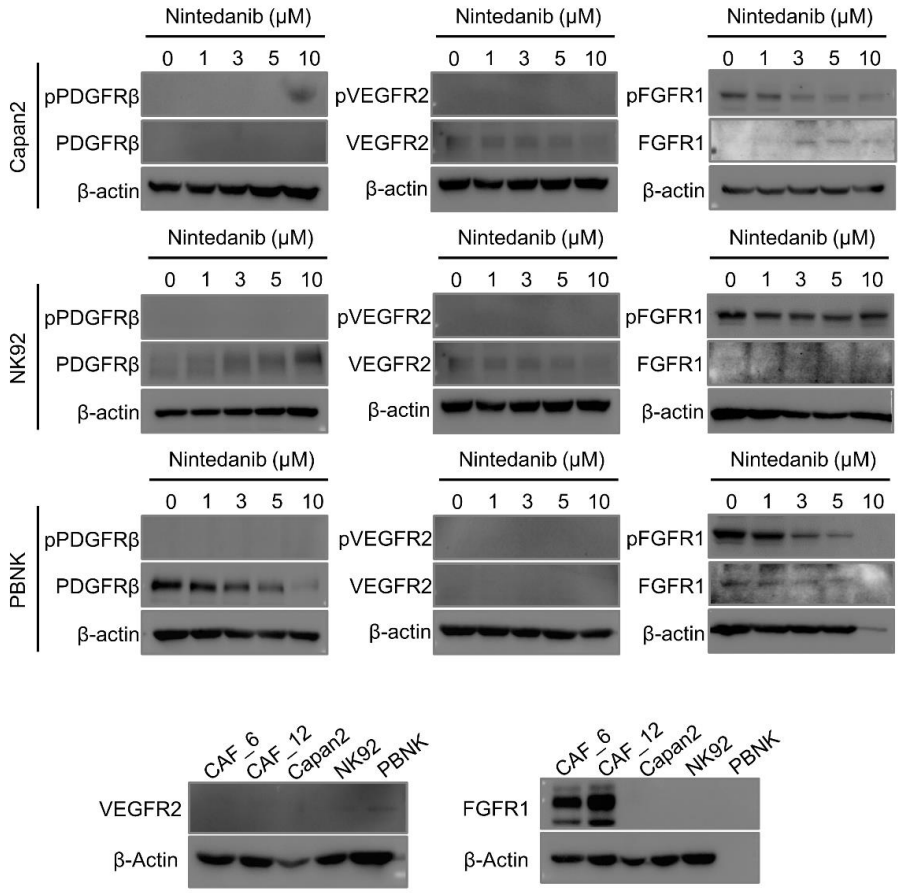


**Supplemental Figure 3.** Putative molecular targets in response to nintedanib on Capan2 and NK cells were assessed using western blot analysis.

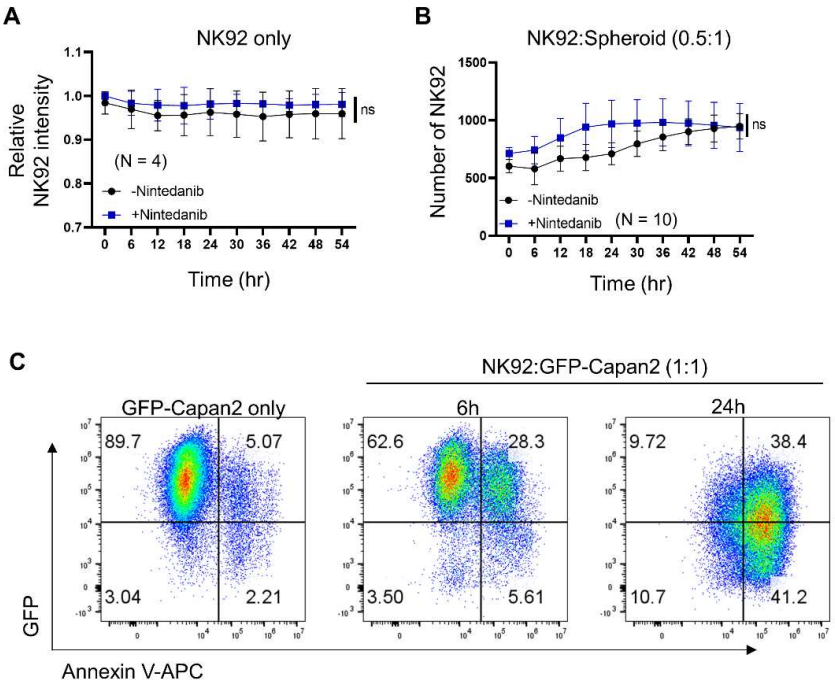


**Supplemental Figure 4.** (A) NK92 cells were tested in the presence or absence of nintedanib, respectively. (B) Number of NK92 cells after co-culture. (C) Annexin V influx was measured on GFP-Capan2 cells to determine apoptotic death.

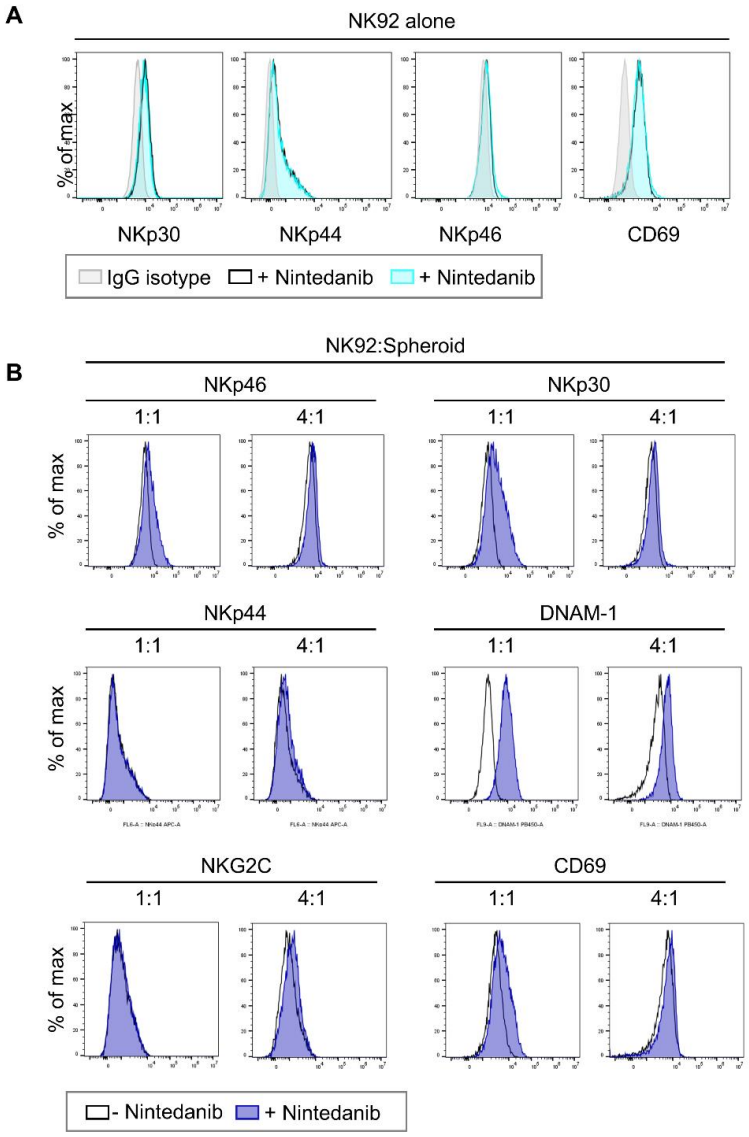


**Supplemental Figure 5.** Expression of activating receptors on NK92 cells under nintedanib treatment.

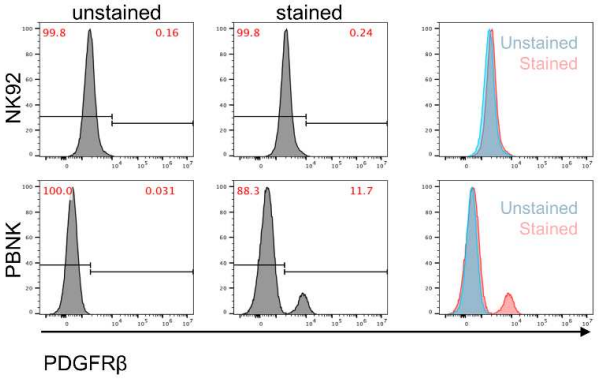


**Supplemental Figure 6.** Surface expression of PDGFRβ on NK cells. To test the level of expression of PDGFRβ on NK cells, flow cytometry was conducted on NK92 and PBNK cells.

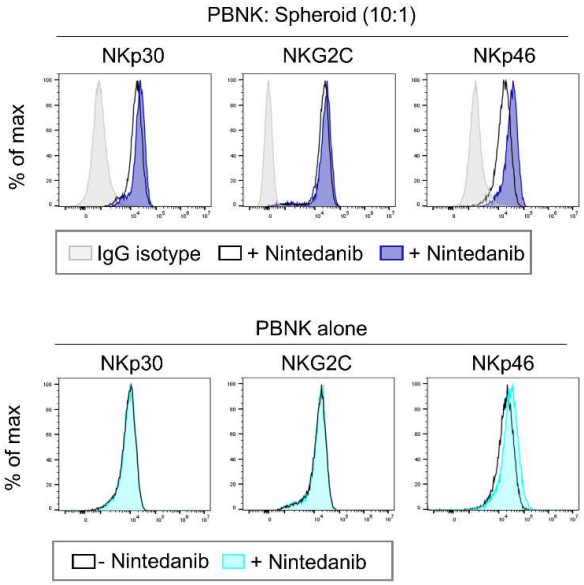


**Supplemental Figure 7.** Expression of activating receptors on PBNK cells under nintedanib treatment.

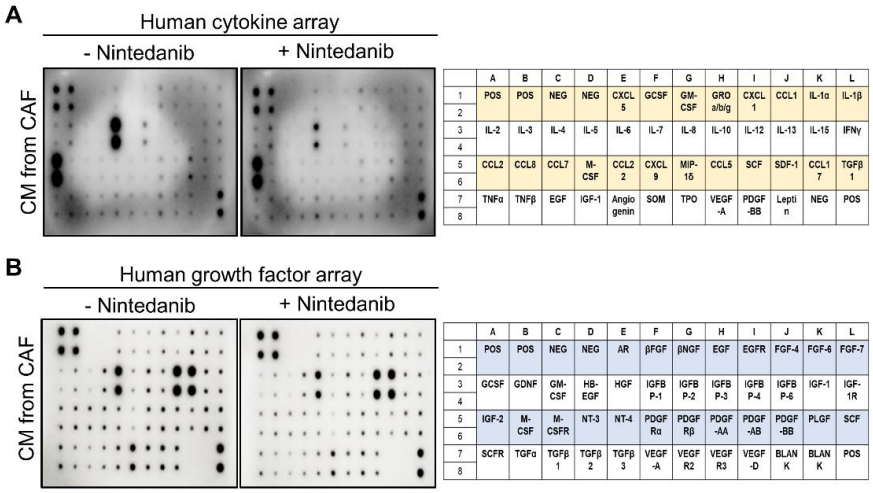


| | A | B | C | D | E | F | G | H | I | J | K | L |
|---|---|---|---|---|---|---|---|---|---|---|---|---|
| 1 | POS | POS | NEG | NEG | CXCL 5 | GCSF | GM-CSF | GRO a/b/g | CXCL 1 | CCL1 | IL-1α | IL-1β |
| 2 | | | | | | | | | | | | |
| 3 | IL-2 | IL-3 | IL-4 | IL-5 | IL-6 | IL-7 | IL-8 | IL-10 | IL-12 | IL-13 | IL-15 | IFNγ |
| 4 | | | | | | | | | | | | |
| 5 | CCL2 | CCL8 | CCL7 | M-CSF | CCL2 2 | CXCL 9 | MIP-1δ | CCL5 | SCF | SDF-1 | CCL1 7 | TGFβ 1 |
| 6 | | | | | | | | | | | | |
| 7 | TNFα | TNFβ | EGF | IGF-1 | Angio genin | SOM | TPO | VEGF -A | PDGF -BB | Lepti n | NEG | POS |
| 8 | | | | | | | | | | | | |

| | A | B | C | D | E | F | G | H | I | J | K | L |
|---|---|---|---|---|---|---|---|---|---|---|---|---|
| 1 | POS | POS | NEG | NEG | AR | βFGF | βNGF | EGF | EGFR | FGF-4 | FGF-6 | FGF-7 |
| 2 | | | | | | | | | | | | |
| 3 | GCSF | GDNF | GM-CSF | HB-EGF | HGF | IGFB P-1 | IGFB P-2 | IGFB P-3 | IGFB P-4 | IGFB P-6 | IGF-1 | IGF-1R |
| 4 | | | | | | | | | | | | |
| 5 | IGF-2 | M-CSF | M-CSFR | NT-3 | NT-4 | PDGF Rα | PDGF Rβ | PDGF -AA | PDGF -AB | PDGF -BB | PLGF | SCF |
| 6 | | | | | | | | | | | | |
| 7 | SCFR | TGFα | TGFβ 1 | TGFβ 2 | TGFβ 3 | VEGF -A | VEGF R2 | VEGF R3 | VEGF -D | BLAN K | BLAN K | POS |
| 8 | | | | | | | | | | | | |

**Supplemental Figure 8.** Analysis of CAF-released secretome upon treatment with nintedanib. CAFs were treated with or without 3 μM nintedanib, and CAF-derived conditioned media (CM) were harvested 48 h (A) or 72 h (B) post treatment, respectively. Subsequently, human cytokine (A) and growth factor (B) proteins were detected in CM.

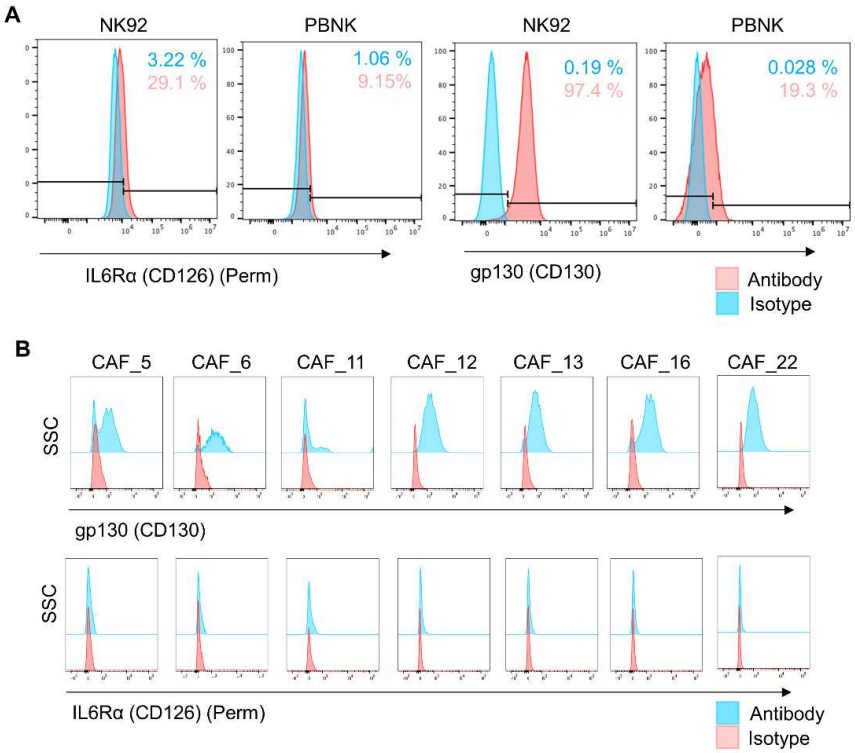


**Supplemental Figure 9.** Expression of IL-6 receptors in NK cells and CAFs, analyzed by flow cytometry. For detection of membrane-bound and soluble IL-6Rα, intercellular staining was performed.

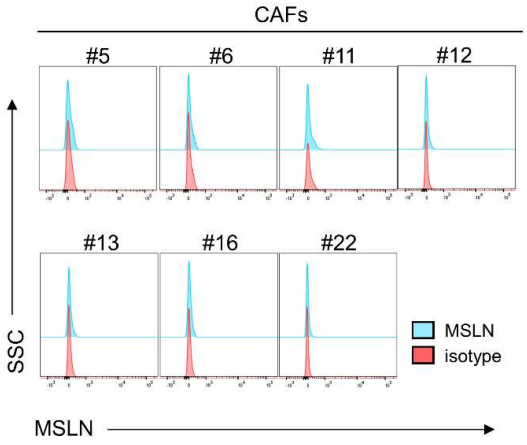

**Supplemental Figure 10.** Expression of MSLN on CAFs was evaluated by flow cytometry.

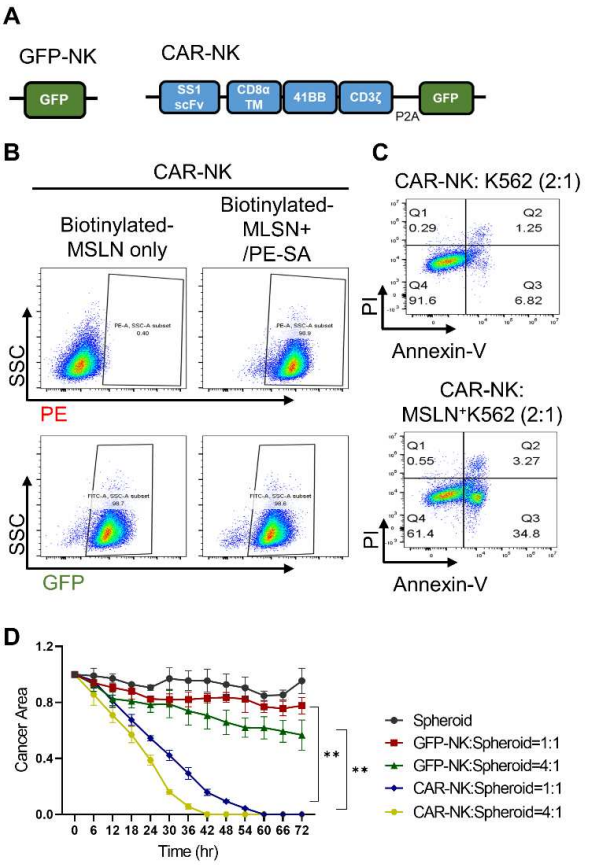


**Supplemental Figure 11.** Generation of MSLN-targeted CAR-NK. (A) GFP-NK and CAR-NK vector constructs. (B) The expression of SS1 scFv-carrying CAR was confirmed using FACS analysis. (C) The antigen-dependent cell killing of CAR-NK was tested in a coculture with K562 or MSLN$^{+}$ K562 cells, respectively. Cancer killing efficacy was evaluated using an Annexin-V/PI staining kit. (D) Time-dependent tumor killing of GFP-NK or CAR-NK was conducted in an *in-vitro* Capan2-CAF spheroid system. For live cell imaging, GFP-expressing Capan2 cells were used and the cancer area was quantified from the GFP fluorescence signal in an automated live cell microscope using the Gen5 Software.

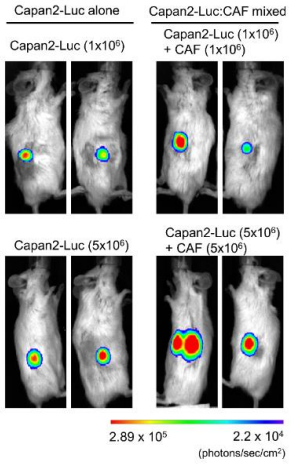


**Supplemental Figure 12.** Comparison of tumor growth in tumor- and tumor/CAF-bearing xenograft mice. Capan2-Luc alone or a mixture of Capan2-Luc and CAF was subcutaneously injected into immune-deficient NSG mice, respectively. For monitoring tumor growth, the *in-vivo* luminescence signal from Capan2-Luc cells was detected by an intravenous injection of substrate on each xenograft mouse using the IVIS imaging system.

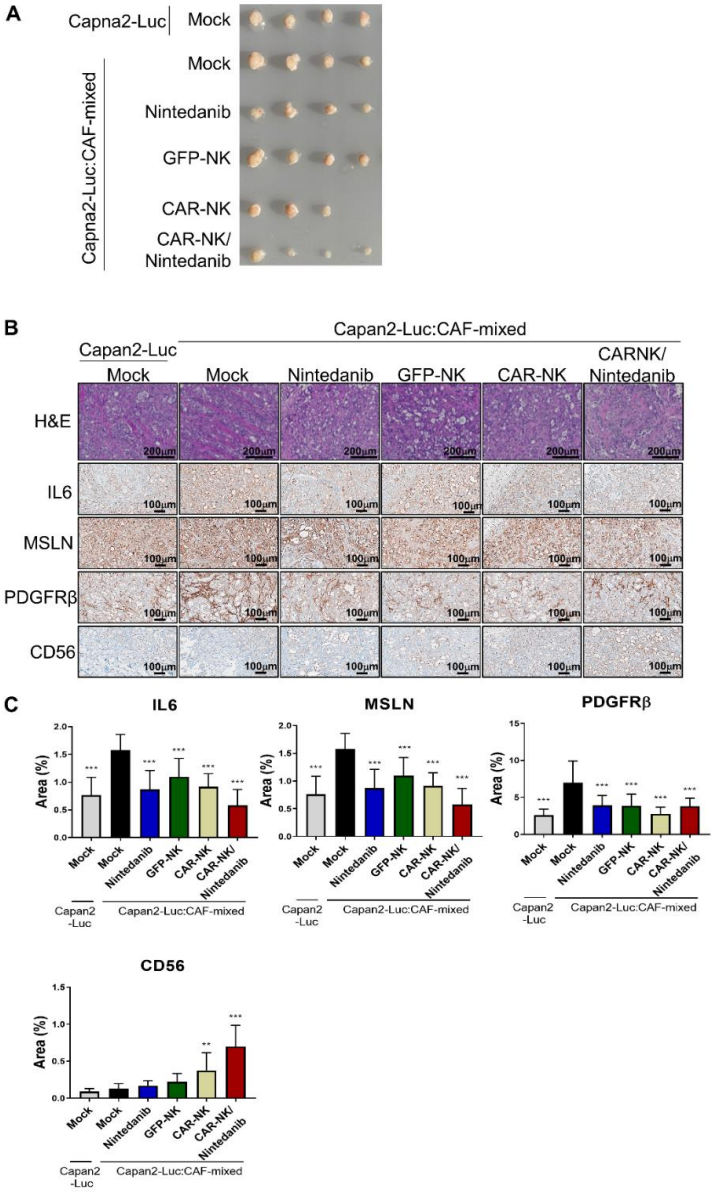


**Supplemental Figure 13.** (A) The tumor tissues in each treatment group were obtained at 34 d post tumor implantation. Combinatory treatment with nintedanib achieved synergistic cytotoxic effects of CAR-NK in Capan2-Luc:CAF-mixed xenograft mice. (B,C) Histological analysis and IHC staining were conducted in excised tumor sections. The IHC staining tissues were scanned with a VS200 slide scanner and the stained areas were quantified using the HALO platform.

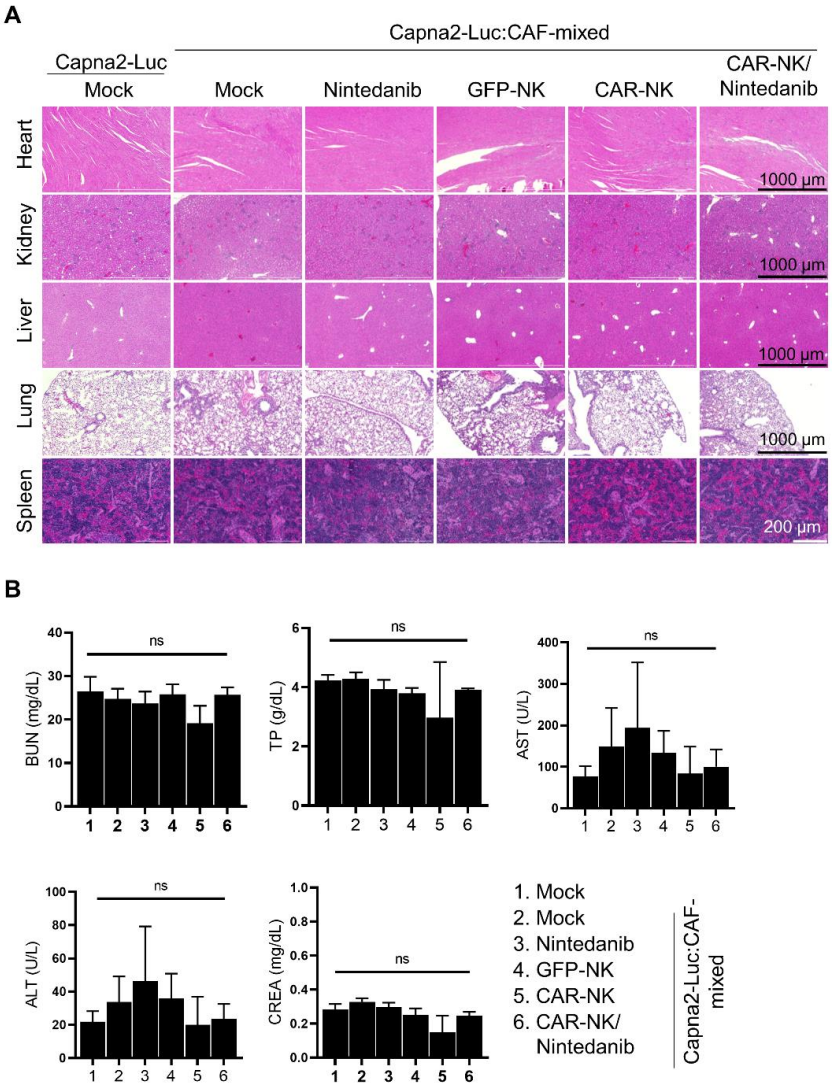


**Supplemental Figure 14.** Off-tumor toxicity was determined through histological analysis and evaluation of hematologic parameters. (A) Histological observations in H&E-stained normal tissues, including the heart, kidney, liver, lung, and spleen obtained from each group. (B) Various hematological parameters were measured in the blood of mice. BUN: blood urea nitrogen, TP: total protein, AST: aspartate aminotransferase, ALT: alanine aminotransferase, CREA: creatinine.

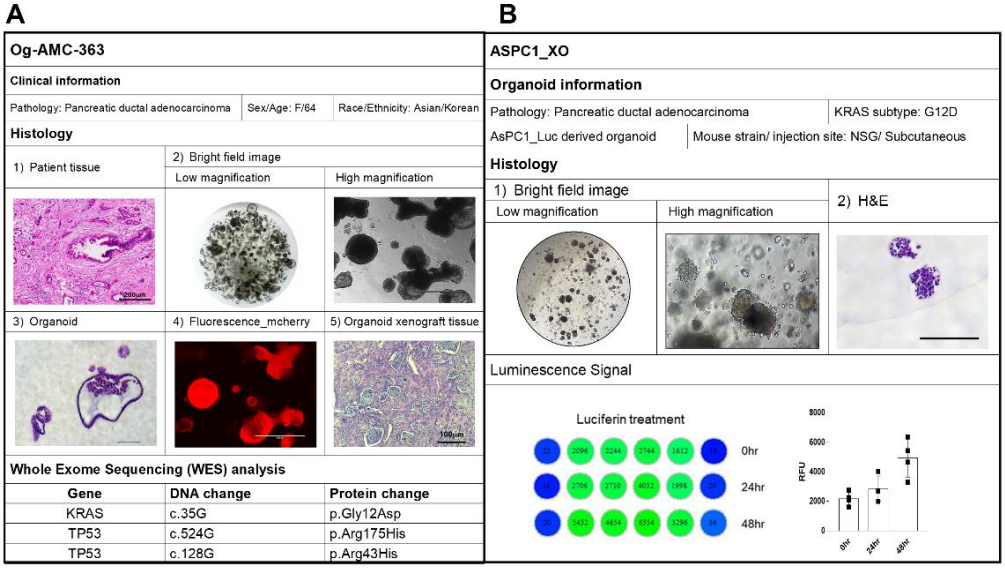


**Supplemental Figure 15.** Characterization of (A) patient- or (B) cancer cell line-derived organoids.

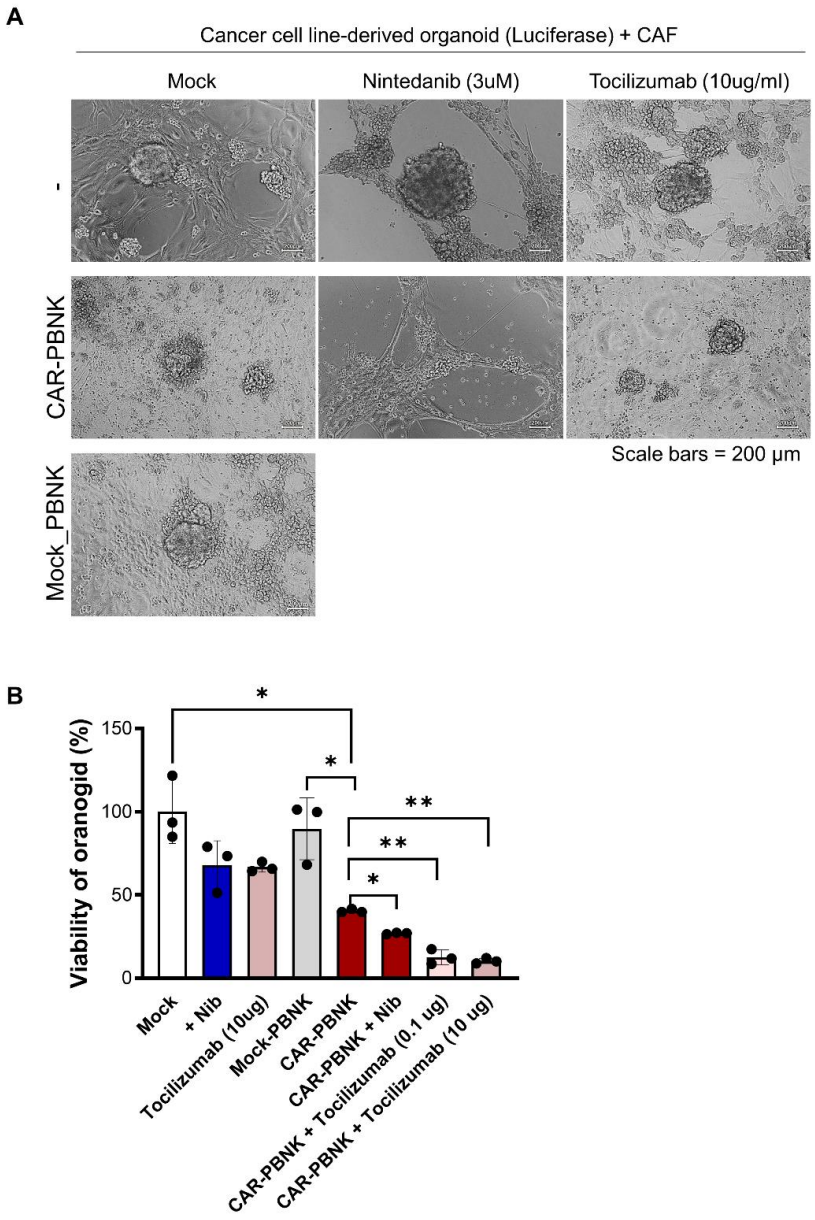


**Supplemental Figure 16.** Synergistically combinatory therapeutic effects in the cancer cell line-derived organoid/CAF co-culture system. The cell killing of CAR-PBNK was assessed under nintedanib treatment or IL-6R blocking antibody (tocilizumab) in a luciferase-expressing organoid/CAF co-culture system. Organoid, CAF, and CAR-PBNK were co-cultured at the ratio of 1:1:4. Organoid killing efficacy was evaluated by detection of the

luminescence signal

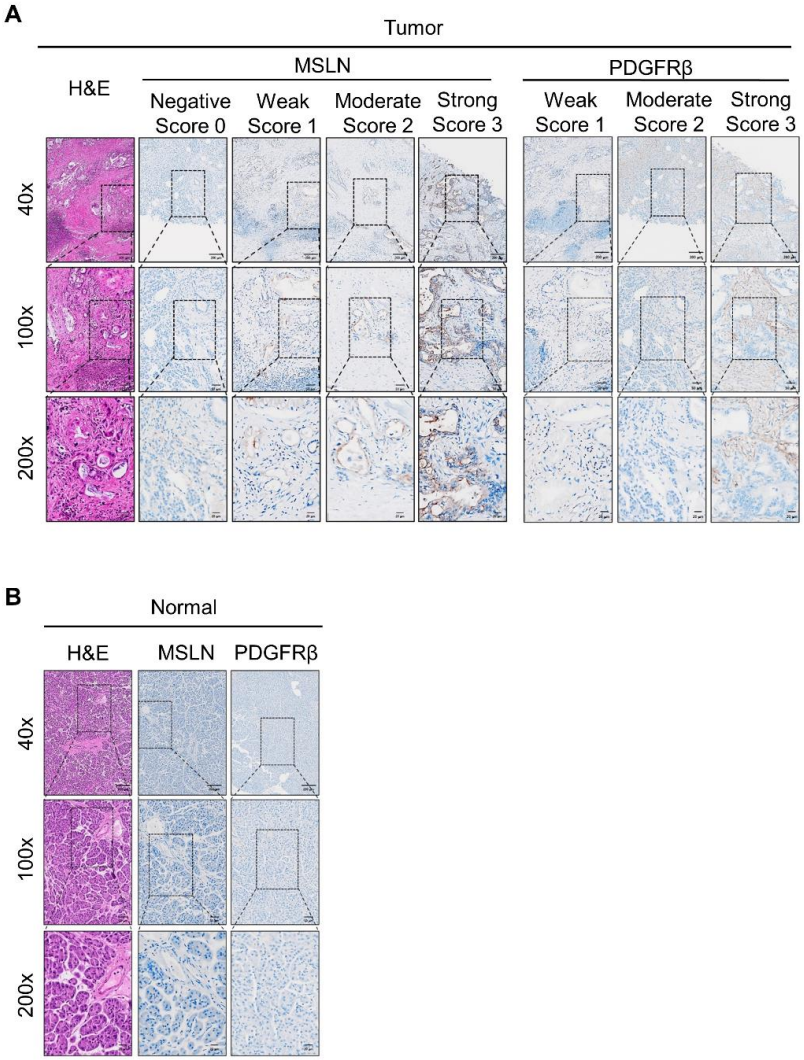


**Supplemental Figure 17.** Expression of MSLN and PDGFRβ on tumor and normal tissues in patient-derived pancreatic cancer. H&E and IHC staining were conducted on tumor (A) and normal tissues (B). (A) Based on IHC staining intensity, the expression score was classified from 0 to 3, with the degree of intensity being regrouped into low and high. (B) Expression of MSLN and PDGFRβ on normal tissues. Size bars indicate 200, 50, and 20 μm at 40×, 100×, and 200× magnification, respectively.

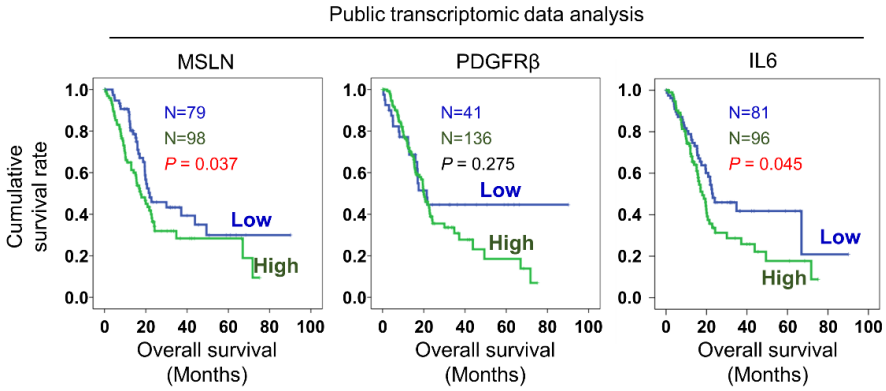


**Supplemental Figure 18.** Survival analysis related with the mRNA expression of MSLN, PDGFRβ, and IL-6 in pancreatic cancer tissues based on cBioportal public data. On the cBioportal site (http://www.cbioportal.org), the PanCancer data set was divided into three groups according to the mRNA expression of MSLN, PDGFRβ, and IL-6, and the overall survival was analyzed based on the level of expression; MSLN-Low (N = 79), High (N = 98); PDGFRβ- Low (N = 41), High (N = 136); IL-6-Low (N = 81), High (N = 96). N indicates the number of samples.

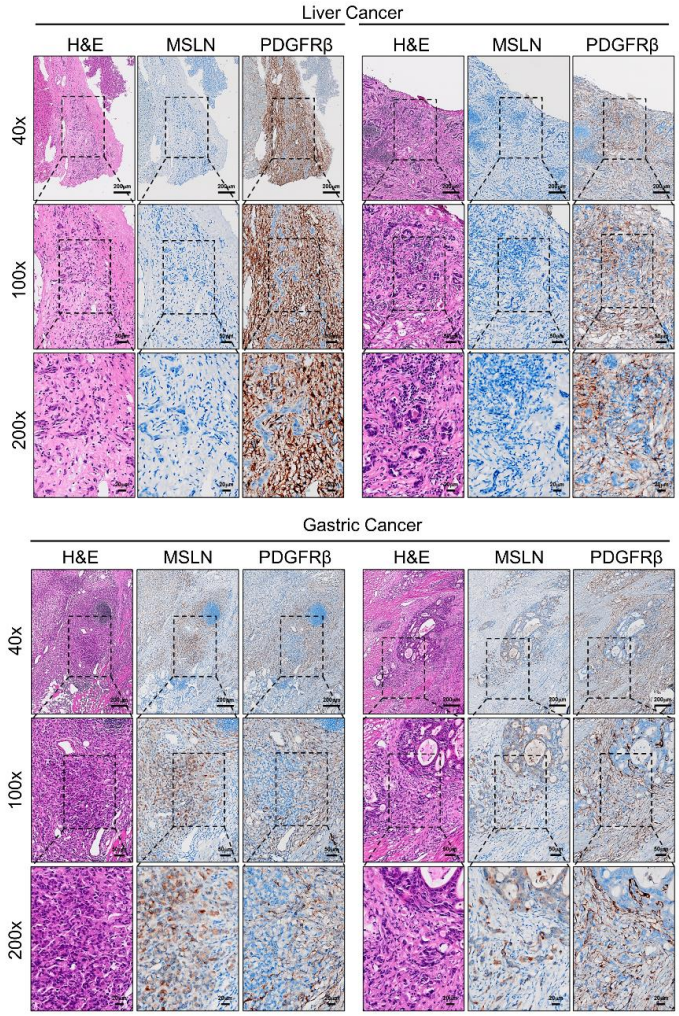


**Supplemental Figure 19.** Expression of MSLN and PDGFRβ on tumor tissues in patient-derived liver and gastric cancer, respectively. For detection of each marker, IHC staining was performed on tumor sections from two independent clinical specimens. For histological observation, H&E staining was independently conducted in the same sections. As expected, MSLN was mainly expressed in tumor cells, whereas PDGFRβ was expressed in the stromal region. Size bars indicate 200, 50, and 20 μm at 40×, 100×, and 200× magnification, respectively.

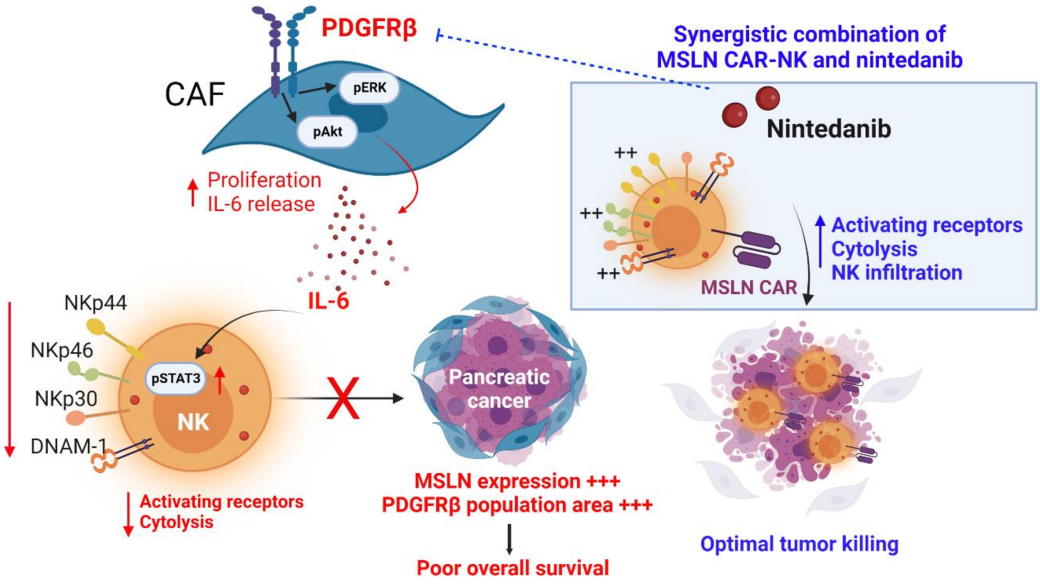


**Supplemental Figure 20.** Working mechanism for therapeutic combination of MSLN CAR-NK and nintedanib in PDAC. The combination of expression of MSLN and the PDGFRβ$^{+}$ population area was involved in unfavorable clinical outcomes with poor overall survival. In PDGFRβ$^{+}$ CAFs, high amounts of IL-6 were secreted via PDGFRβ-mediated signal transduction; consequently, paracrine IL-6 attenuated the NK cytotoxic function through inhibition of pSTAT3-mediated activating receptors. Here we demonstrated that nintedanib inhibited CAF-derived IL-6, rescued NK function, and showed significantly enhanced tumor killing *in vitro* and *in vivo*. In our Capan2-CAF mixed xenograft mice, combination with nintedanib significantly ameliorated CAR-NK-driven cytolysis against MSLN-expressing cancer followed by enhanced NK infiltration. Thus, our synergistic combination of MSLN CAR NK and nintedanib might provide a promising therapeutic option for PDAC. The conceptual figure was created with BioRender.com.

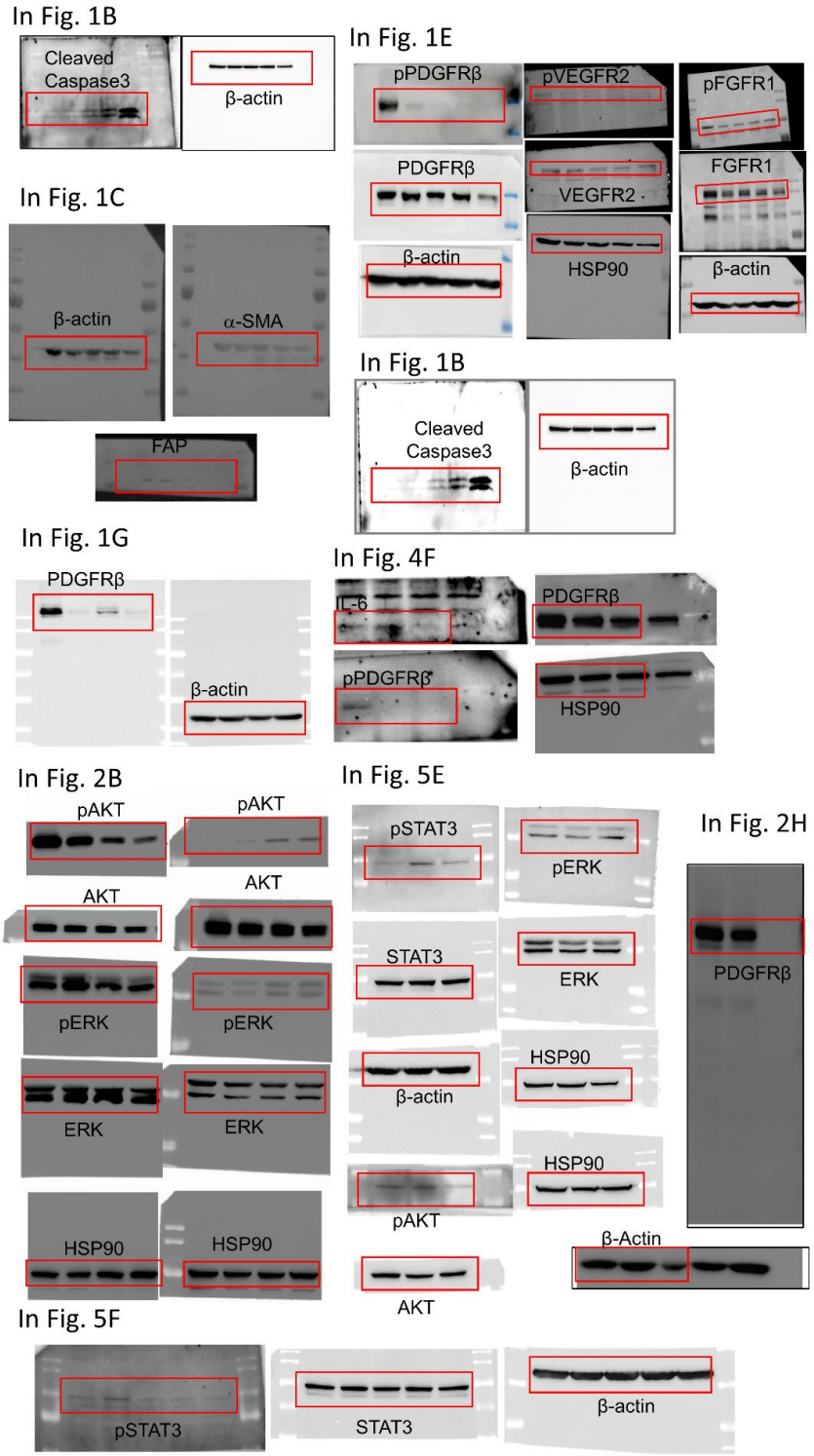


**Supplemental Figure 21.** Full western blots used in the main figures.

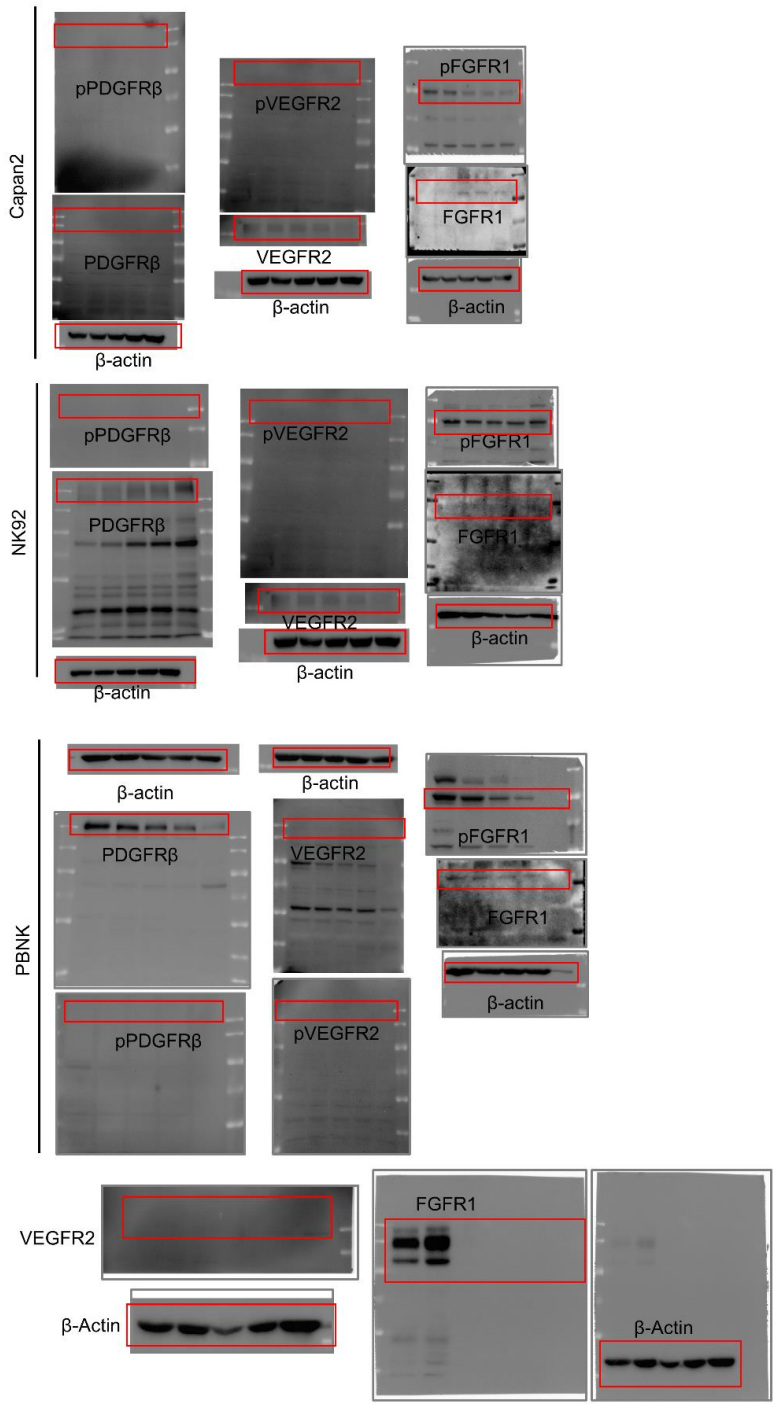


**Supplemental Figure 22.** Full western blots used in online supplemental figure S3.

**Supplemental Table 1.** Clinical information of patient derived cancer-associated fibroblasts (CAFs). DPS; distal pancreatectomy and splenectomy, PDAC; Pancreas ductal adenocarcinoma, LVI; Lympho-vascular Invasion, PNI; Peri-neural Invasion, LN; Lymph node

| ID | Pathologic finding | | | | | | | | |
|---|---|---|---|---|---|---|---|---|---|
| | Operation | Pathology | Tumor size (cm) | Tumor diff-erentiation | LVI | PNI | LN metastasis | No of NL metastasis | TNM stage |
| CAF_11 | DPS | PDAC | 2.6 | moderate | positive | positive | positive | 2 | T2N1M0 (IIB) |
| CAF_12 | DPS | PDAC | 2.8 | moderate | negative | positive | negative | 0 | T2N0M0 (IB) |
| CAF_13 | DPS | PDAC | 6.1 | moderate | positive | positive | positive | 1 | T3N1M0 (IIB) |
| CAF_16 | DPS | PDAC | 3.7 | moderate | positive | positive | negative | 0 | T2N0M0 (IB) |
| CAF_22 | DPS | PDAC | 4.5 | moderate | positive | positive | positive | 2 | T3N0M0 (IIA) |

**Supplemental Table 2.** Clinico-pathological characteristics of enrolled patients. PD; pancreaticoduodenectomy, TPS; total pancreatectomy with splenectomy, DPS; distal pancreatectomy with splenectomy

| Factors | | Values |
|---|---|---|
| Age (y) | Avg. ± SD (range) | 60.4±9.5 (32 -78) |
| Sex (Female/Male) | N (%) | 12/31 (27.9%/72.1%) |

| Operation and Pathologic findings | | | |
|---|---|---|---|
| | PD/DPS/TPS | N (%) | 18/23/2 (41.9% /53.5%/4.6%) |
| | Turmo size (cm) | Avg. ± SD (range) | 3.5±1.6 (1.4-9.0) |
| | Differentiation (wel/mod/por) | N (%) | 4/34/5 (9.3%/79.1%/11.6%) |
| | T stage (T1/T2/T3/T4) | N (%) | 4/27/10/2 (9.3%/62.8%/23.3%/4.6%) |
| | N stage (N0/N1/N2) | N (%) | 18/19/6 (41.9%/44.2%/13.9%) |

**Supplemental Table 3.** Expression score based on the IHC staining intensity and the area of expression of PDGFRβ and IL-6 in tumor tissues. The intensity of expression for MSLN and PDGFRβ was analyzed by the pathologist who was specialized in pancreatic cancer, and scored on a scale from 0 to 3; MSLN-score 0 (N = 16), score 1 (N = 7), score 2 (N = 8), score 3 (N = 12); PDGFRβ-score 0 (N = 0), score 1 (N = 6), score 2 (N = 10), score 3 (N = 27). After scanning of each slide with the VS200 research slide scanner, the staining range of PDGFRβ and IL-6 was automatically quantified.

| ID | MSLN_Score | PDGFRβ_Score | PDGFRβ _PA (%) | IL-6_PA (%) |
|---|---|---|---|---|
| PDAC_01 | 1 | 3 | 15.11 | 17.6 |
| PDAC_02 | 0 | 2 | 4.85 | 6.85 |
| PDAC_03 | 1 | 1 | 0.57 | 20.78 |
| PDAC_04 | 0 | 3 | 28.76 | 12.65 |
| PDAC_05 | 0 | 3 | 6.58 | 10.65 |
| PDAC_06 | 0 | 3 | 15.91 | 14.20 |
| PDAC_07 | 3 | 3 | 12.84 | 10.28 |

| | | | | |
|---|---|---|---|---|
| PDAC_08 | 3 | 3 | 3.77 | 19.31 |
| PDAC_09 | 3 | 3 | 32.67 | 21.79 |
| PDAC_10 | 2 | 1 | 2.46 | 11.07 |
| PDAC_11 | 3 | 2 | 2.98 | 64.72 |
| PDAC_12 | 0 | 3 | 17.20 | 19.34 |
| PDAC_13 | 1 | 1 | 1.23 | 25.65 |
| PDAC_14 | 2 | 3 | 4.12 | 21.58 |
| PDAC_15 | 2 | 2 | 5.71 | 19.66 |
| PDAC_16 | 0 | 2 | 4.51 | 20.42 |
| PDAC_17 | 3 | 3 | 18.08 | 27.16 |
| PDAC_18 | 0 | 3 | 13.55 | 23.16 |
| PDAC_19 | 0 | 3 | 7.28 | 4.91 |
| PDAC_20 | 0 | 2 | 3.55 | 29.16 |
| PDAC_21 | 2 | 3 | 5.09 | 23.45 |
| PDAC_22 | 3 | 3 | 4.33 | 11.67 |
| PDAC_23 | 0 | 3 | 13.99 | 9.69 |
| PDAC_24 | 2 | 2 | 8.83 | 16.28 |
| PDAC_25 | 0 | 2 | 9.52 | 7.58 |
| PDAC_26 | 3 | 3 | 4.66 | 16.37 |
| PDAC_27 | 3 | 3 | 1.48 | 11.01 |
| PDAC_28 | 0 | 3 | 6.47 | 11.15 |
| PDAC_29 | 2 | 3 | 10.78 | 16.51 |
| PDAC_30 | 1 | 3 | 3.60 | 30.80 |
| PDAC_31 | 2 | 2 | 4.64 | 13.22 |
| PDAC_32 | 3 | 2 | 2.44 | 10.15 |
| PDAC_33 | 3 | 3 | 7.73 | 16.01 |
| PDAC_34 | 0 | 3 | 10.21 | 9.06 |
| PDAC_35 | 3 | 3 | 4.06 | 13.66 |
| PDAC_36 | 3 | 3 | 12.35 | 25.09 |
| PDAC_37 | 1 | 1 | 3.43 | 6.78 |
| PDAC_38 | 1 | 1 | 9.41 | 10.85 |
| PDAC_39 | 1 | 2 | 2.79 | 8.74 |
| PDAC_40 | 0 | 3 | 12.14 | 10.71 |
| PDAC_41 | 0 | 1 | 2.37 | 10.60 |
| PDAC_42 | 0 | 3 | 14.50 | 9.05 |
| PDAC_43 | 2 | 3 | 15.70 | 26.01 |

**Supplemental Table 4.** List of primers used for qRT-PCR analysis

| Target | Forward primer | Reverse primer |
|---|---|---|
| **IL-6** | AATTCGGTACATCCTCGACGG | TTGGAAGGTTCAGGTTGTTTTCT |
| **18s** | GCCTGAGAAACGGCTACCA | GTCGGGAGTGGGTAATTTGC |

**Supplemental table 4** List of primers used for qRT-PCR analysis.

**Supplemental Table 5.** Sequence of sgRNA targeting PDGFRβ

| sgRNA | Sequence Reverse primer |
|---|---|
| A | CCCGGTCAAGGACACATGGC |
| B | GGTGGACTATGTGCCCATGC |
| C | ACTACGTTCCCTCTGGTGGG |
| D | TGAGCACGTTCCTAGCCGCC |
| E | AGATTCCCTCCTGACCAGTG |